DE GRUYTER OPEN
DOI: 10.1515/ace-2017-0026
ARCHIVES OF CIVIL ENGINEERING
Vol. LXIII ISSUE 3 2017



# PLATE FINITE ELEMENT WITH PHYSICAL SHAPE FUNCTIONS: CORRECTNESS OF THE FORMULATION

**W. GILEWSKI[1], M. SITEK[2]**

The formulation of a plate finite element with so called 'physical' shape functions is revisited. The derivation of the 'physical' shape functions is based on Hencky-Bollé theory of moderately thick plates. The considered finite element was assessed in the past, and the tests showed that the solution convergence was achieved in a wide range of thickness to in-plane dimensions ratios. In this paper a holistic correctness assessment is presented, which covers three criteria: the ellipticity, the consistency and the inf-sup conditions. Fulfilment of these criteria assures the existence of a unique solution, and a stable and optimal convergence to the correct solution. The algorithms of the numerical tests for each test case are presented and the tests are performed for the considered formulation. In result it is concluded that the finite element formulation passes every test and therefore is a good choice for modeling plate structural elements regardless of their thickness.

*Keywords:* Plate finite element, Physical shape functions, Ellipticity, Consistency, Inf-sup condition

## 1. INTRODUCTION

The development of new finite elements within beam, plate and shell theories is still a very important research topic [1, 2, 3, 4]. One of the most interesting finite element formulations is a rectangular plate finite element with physical shape functions proposed in [5]. The concept of physical shape functions assumes their dependence on the material properties and the geometrical characteristics of the element. These shape functions have a physical interpretation, i.e. they represent displacements and rotations due to imposed unit nodal displacements. The authors of [6]

[1] Prof., DSc., PhD., Eng., Warsaw University of Technology, Faculty of Civil Engineering, Al. Armii Ludowej 16, 00-637 Warsaw, Poland, e-mail: w.gilewski@il.pw.edu.pl

[2] PhD., Eng., Warsaw University of Technology, Faculty of Civil Engineering, Al. Armii Ludowej 16, 00-637 Warsaw, Poland, e-mail" m.sitek@il.pw.edu.pl

performed a series of numerical tests and presented results that prove an excellent convergence of the formulation regardless of the element thickness. However, there is no formal assessment of the formulation's correctness to be found in literature. The unconventional approach used in this formulation is difficult to evaluate by means of typically employed criteria.

In this paper the correctness of the finite element formulation is examined using three criteria: ellipticity, consistency and inf-sup. If these conditions are satisfied, then: a) a unique solution exists, b) the solution converges to the exact one with optimal convergence, and c) the formulation is stable. This set of criteria was first proposed in [7] for mixed formulations, but it can be successfully used for a displacement formulation, as it was shown in [2, 8]. The verification of the ellipticity condition consists of an analysis of eigenvalues of a stiffness matrix of a single unsupported finite element. It is required that the matrix is non-negatively defined, and the eigenvectors corresponding to the calculated eigenvalues represent the correct energy modes, without additional zero-energy modes. If the condition is met, the existence of a unique solution is guaranteed. The convergence of a finite element solution is assured when the consistency condition is met [9]. Various quantities, such as internal energy stored in an element, can be taken as the convergence measure. Based on this assumption an energy criterion for consistency was proposed in [1]. Satisfaction of the inf-sup condition, which was described in detail in [10, 11], guarantees stability of the formulation independently of the finite element mesh used. It also assures an optimal order of the solution convergence. This condition is frequently used by various authors [12, 13, 14, 15]. The inf-sup condition should be verified in several well-chosen test cases. Plate elements tend to show parasitic states in bending-dominated problems, as showed in literature [16, 17, 18, 19, 20], therefore this type of benchmarks is presented in this paper.

## 2. FORMULATION OF THE PLATE FINITE ELEMENT WITH PHYSICAL SHAPE FUNCTIONS

Let us consider a rectangular plate finite element with a formulation based on the Hencky-Bollé theory [21, 22, 23] for moderately thick plates in a Cartesian system of coordinates $x$, $y$. The in-plane dimensions of the element are $2a$ by $2b$ and the thickness is $h$. A dimensionless coordinate system with the origin in the center of the finite element is introduced

$$\xi = \frac{x}{a}, \quad \eta = \frac{y}{b}, \tag{1}$$

with $\xi \in \langle -1,1 \rangle$ and $\eta \in \langle -1,1 \rangle$, and a vector of nodal parameters

$$\mathbf{q} = [\mathbf{q}_1 \ \mathbf{q}_2 \ \mathbf{q}_3 \ \mathbf{q}_4]^{\mathrm{T}}, \ \mathbf{q}_i = [w_i \ \phi_{xi} \ \phi_{yi}]^{\mathrm{T}} \tag{2}$$

where $w_i$ - vertical displacement, $\phi_{xi}$ - rotation angle along $x$ axis, $\phi_{yi}$ - rotation angle along $y$ axis. Figure 1 shows the geometry of the finite element and the adopted local coordinate system along with nodal degrees of freedom.

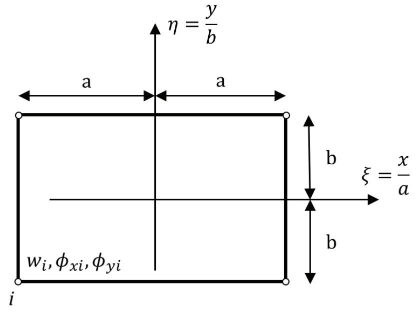


Fig. 1. The considered plate finite element

The considered nonstandard finite element formulation with physical shape functions is based on the idea that the shape functions have a physical interpretation. The shape functions are solutions of the displacement equilibrium equations of a Hencky-Bollé plate strips with unit boundary conditions. The derivation is presented in [5, 6].

The shape function matrix $\mathbf{N}$ is expressed as

$$\mathbf{N} = [\mathbf{N}_1 \ \mathbf{N}_2 \ \mathbf{N}_3 \ \mathbf{N}_4]^{\mathrm{T}}, \quad \mathbf{N}_i(\xi,\eta) = \begin{bmatrix} w_x^{iw}(\xi)\cdot w_y^{iw}(\eta) & a\cdot w_x^{i\phi}(\xi)\cdot w_y^{iw}(\eta) & b\cdot w_x^{iw}(\xi)\cdot w_y^{i\phi}(\eta) \\ \frac{1}{a}\phi_x^{iw}(\xi)\cdot w_y^{iw}(\eta) & \phi_x^{i\phi}(\xi)\cdot w_y^{iw}(\eta) & \frac{b}{a}\phi_x^{iw}(\xi)\cdot w_y^{i\phi}(\eta) \\ \frac{1}{b}w_x^{iw}(\xi)\cdot \phi_y^{iw}(\eta) & \frac{a}{b}w_x^{i\phi}(\xi)\cdot \phi_y^{iw}(\eta) & w_x^{iw}(\xi)\cdot \phi_y^{i\phi}(\eta) \end{bmatrix} \tag{3}$$

with

$$
\begin{aligned}
& w_x^{iw}(\xi) = \rho(\xi_i\xi) - \mu_x \chi(\xi_i\xi), && w_y^{iw}(\eta) = \rho(\eta_i\eta) - \mu_y \chi(\eta_i\eta), \\
& w_x^{i\phi}(\xi) = \xi_i\left[\omega(\xi_i\xi) - \mu_x \chi(\xi_i\xi)\right], && w_y^{i\phi}(\eta) = \eta_i\left[\omega(\eta_i\eta) - \mu_y \chi(\eta_i\eta)\right], \qquad i=1,2,3,4, \\
& \phi_x^{iw}(\xi) = -\xi_i(1-\mu_x)\rho^I(\xi_i\xi), && \phi_y^{iw}(\eta) = -\eta_i(1-\mu_y)\rho^I(\eta_i\eta), \\
& \phi_x^{i\phi}(\xi) = -\omega^I(\xi_i\xi) + \mu_x \rho^I(\xi_i\xi), && \phi_y^{i\phi}(\eta) = -\omega^I(\eta_i\eta) + \mu_y \rho^I(\eta_i\eta),
\end{aligned} \tag{4}
$$

where for isotropic material

$$
\mu_x = \frac{3\gamma_x}{1+3\gamma_x}, \; \mu_y = \frac{3\gamma_y}{1+3\gamma_y}, \; \gamma_x = \frac{D}{Ha^2}, \; \gamma_y = \frac{D}{Hb^2},
$$

$$
\rho(\xi) = \frac{1}{4}(2+3\xi-\xi^3), \quad \omega(\xi) = \frac{1}{4}(1+\xi-\xi^2-\xi^3), \quad \chi(\xi) = \frac{1}{4}(\xi-\xi^3), \tag{5}
$$

$$
\xi_1 = -1, \quad \xi_2 = 1, \quad \xi_3 = 1, \quad \xi_4 = -1, \quad \eta_1 = -1, \quad \eta_2 = -1, \quad \eta_3 = 1, \quad \eta_4 = 1
$$

and $D = \dfrac{Eh^3}{12(1-\nu^2)}$ - bending stiffness, $H = \dfrac{kEh}{2(1+\nu)}$ - shear stiffness, $E$ – Young’s modulus, ν - Poisson’s ratio, $k$ – shear coefficient.

The stiffness matrix and the load vector are obtained following the standard finite element procedure, presented in [13] among others. Calculation of these matrices is performed with the use of the exact integration. The stiffness matrix elements are as following

$$
\mathbf{K}^e = \left[\mathbf{K}^e_{ij}\right], \; \mathbf{K}^e_{ij} = \left[k_{ij}^{kl}\right], \; i,j = 1,2,3,4, \;\; k,l = 1,2,3, \tag{6}
$$

$$
k_{ij}^{11} = \frac{D}{ab}\frac{\xi_i\xi_j\eta_i\eta_j}{700}\left\{
\begin{aligned}
& 5\frac{b^2}{a^2}(1-\mu_x)\left(105\eta_i\eta_j + 51 - 18\mu_y + 2\mu_y^2\right) + \\
& + 5\frac{a^2}{b^2}(1-\mu_y)\left(105\xi_i\xi_j + 51 - 18\mu_x + 2\mu_x^2\right) + \\
& + 21(1-\nu)\left[(1-\mu_x)^2\left(6-2\mu_y+\mu_y^2\right) + (1-\mu_y)^2\left(6-2\mu_x+\mu_x^2\right)\right] + \\
& + 7(1+\nu)(6-7\mu_x+\mu_x^2)(6-7\mu_y+\mu_y^2)
\end{aligned}
\right\}
$$

$$
k_{ij}^{12}=\frac{D}{b}\frac{\xi_i\eta_i\eta_j}{700}\left\{\begin{array}{l}
5\dfrac{b^2}{a^2}(1-\mu_x)\left(105\eta_i\eta_j+51-18\mu_y+2\mu_y^2\right)+\\
+5\dfrac{a^2}{b^2}(1-\mu_y)\left(35\xi_i\xi_j+9-11\mu_x+2\mu_x^2\right)+\\
+7\dfrac{1-\nu}{2}(1-\mu_x)\left[(1-6\mu_x)\left(6-2\mu_y+\mu_y^2\right)+6(1-\mu_x)(1-\mu_y)^2\right]+\\
+7(1-\mu_y)(6-\mu_y)\left[5\nu\left(1+\xi_i\xi_j\right)+\dfrac{1+\nu}{2}\left(2-9\mu_x+2\mu_x^2\right)\right]
\end{array}\right\}
$$

$$
k_{ij}^{13}=\frac{D}{a}\frac{\eta_i\xi_i\xi_j}{700}\left\{\begin{array}{l}
5\dfrac{a^2}{b^2}(1-\mu_y)\left(105\xi_i\xi_j+51-18\mu_x+2\mu_x^2\right)+\\
+5\dfrac{b^2}{a^2}(1-\mu_x)\left(35\eta_i\eta_j+9-11\mu_y+2\mu_y^2\right)+\\
+7\dfrac{1-\nu}{2}(1-\mu_y)\left[(1-6\mu_y)\left(6-2\mu_x+\mu_x^2\right)+6(1-\mu_y)(1-\mu_x)^2\right]+\\
+7(1-\mu_x)(6-\mu_x)\left[5\nu\left(1+\eta_i\eta_j\right)+\dfrac{1+\nu}{2}\left(2-9\mu_y+2\mu_y^2\right)\right]
\end{array}\right\}
$$

$$
k_{ij}^{22}=\frac{Da}{b}\frac{\eta_i\eta_j}{2100}\left\{\begin{array}{l}
5\dfrac{b^2}{a^2}\left[\xi_i\xi_j+3(1-\mu_x)\right]\left(105\eta_i\eta_j+51-18\mu_y+2\mu_y^2\right)+\\
+30\dfrac{a^2}{b^2}\left[7\xi_i\xi_j+(1-\mu_x)^2\right](1-\mu_y)+\\
+14\dfrac{1+\nu}{2}(1-\mu_y)(6-\mu_y)\left[5\xi_i\xi_j+3(1-\mu_x)^2\right]+\\
+7\dfrac{1-\nu}{2}\left[\begin{array}{l}5\xi_i\xi_j\left(12-14\mu_y+7\mu_y^2\right)+36(1-\mu_x)^2(1-\mu_y)^2+\\+90\mu_x^2+15\mu_y(1-2\mu_x)(2-\mu_y)\end{array}\right]
\end{array}\right\}
$$

$$
k_{ij}^{23}=D\frac{\eta_i\xi_j}{700}\left\{\begin{array}{l}
5\dfrac{a^2}{b^2}(1-\mu_y)\left(35\xi_i\xi_j+9-11\mu_x+2\mu_x^2\right)+5\dfrac{b^2}{a^2}(1-\mu_x)\left(35\eta_i\eta_j+9-11\mu_y+2\mu_y^2\right)+\\
+35\nu\left[5\left(1+\xi_i\xi_j\right)\left(1+\eta_i\eta_j\right)+\left(1+\xi_i\xi_j\right)\left(1-7\mu_y+\mu_y^2\right)+\left(1+\eta_i\eta_j\right)\left(1-7\mu_x+\mu_x^2\right)\right]\\
+7\dfrac{1+\nu}{2}\left[(1-\mu_x)^2(1-\mu_y)^2+\left(1-7\mu_x+\mu_x^2\right)\left(1-7\mu_y+\mu_y^2\right)\right]+\\
+7\dfrac{1-\nu}{2}(1-\mu_x)(1-\mu_y)\left[2-7\left(\mu_x+\mu_y\right)+12\mu_x\mu_y\right]
\end{array}\right\}
$$

$$k_{ij}^{33}=\frac{Db}{a}\frac{\xi_i\xi_j}{2100}\left\{\begin{array}{l}5\frac{a^2}{b^2}\left[\eta_i\eta_j+3(1-\mu_y)\right]\left(105\xi_i\xi_j+51-18\mu_x+2\mu_x^2\right)+\\+30\frac{b^2}{a^2}\left[7\eta_i\eta_j+(1-\mu_y)^2\right](1-\mu_x)+14\frac{1+\nu}{2}(1-\mu_x)(6-\mu_x)\left[5\eta_i\eta_j+3(1-\mu_y)^2\right]+\\+7\frac{1-\nu}{2}\left[\begin{array}{l}5\eta_i\eta_j\left(12-14\mu_x+7\mu_x^2\right)+36(1-\mu_x)^2(1-\mu_y)^2+\\+90\mu_y^2+15\mu_x(1-2\mu_y)(2-\mu_x)\end{array}\right]\end{array}\right\}$$

$$k_{ij}^{21}=\xi_i\xi_i k_{ij}^{12},\quad k_{ij}^{31}=\eta_i\eta_j k_{ij}^{13},\quad k_{ij}^{32}=\xi_i\xi_i\eta_i\eta_j k_{ij}^{23}.$$

# 3. VERIFICATION OF THE FORMULATION

## 3.1. ELLIPTICITY CONDITION

It can be shown that verification of the ellipticity condition for a finite element is equal to performing a spectral analysis of a stiffness matrix of an unsupported finite element [9]. The eigenvalue problem considered here is

$$\left(\mathbf{K}^e-\lambda_k\mathbf{I}\right)\mathbf{q}^e=\mathbf{0}. \tag{7}$$

The ellipticity condition states that matrix $\mathbf{K}^e$ is required to be non-negatively defined. There should be as many zero eigenvalues as rigid motions in the theory. The remaining eigenvalues are required to be positive. Eigenvectors corresponding to zero eigenvalues should reproduce rigid motions, and those corresponding to positive eigenvalues should represent nonzero deformation states. If the ellipticity condition is not met, then the existence of a finite element solution cannot be guaranteed.

The considered finite element formulation is based on a moderately thick plate theory, but it should also give good results when used in modeling thin plates. Table I presents results of eigenvalue calculations for a case of an unsupported plate finite element with several different values of thickness and constant in-plane dimensions $a$=$b$=1 m, with proportion $h/2a$ from 1/1 to 1/100, and material properties $E=2\cdot10^4$ Pa and ν=0.25.

Table 1. Eigenvalues of the stiffness matrix of an unsupported finite element (dimensions: $2a$ by $2a$ by $h$, with $a$=$b$=1 m; material characteristics: $E=2\cdot 10^4$ Pa, ν=0.25).

| $\frac{h}{2a}=\frac{1}{1}$ | $\frac{h}{2a}=\frac{1}{2}$ | $\frac{h}{2a}=\frac{1}{5}$ | $\frac{h}{2a}=\frac{1}{10}$ | $\frac{h}{2a}=\frac{1}{20}$ | $\frac{h}{2a}=\frac{1}{50}$ | $\frac{h}{2a}=\frac{1}{100}$ |
|---|---|---|---|---|---|---|
| 23097.1 | 6603.86 | 731.555 | 109.045 | 14.2944 | 0.927365 | 0.116147 |
| 23097.1 | 6603.86 | 673.307 | 92.0098 | 11.7761 | 0.758738 | 0.0949335 |
| 17777.8 | 4957.29 | 673.307 | 92.0098 | 11.7761 | 0.758738 | 0.0949335 |
| 13080.5 | 2222.22 | 142.222 | 17.7778 | 2.22222 | 0.142222 | 0.0177778 |
| 10666.7 | 1333.33 | 105.375 | 14.4493 | 1.85116 | 0.119307 | 0.0149283 |
| 7179.44 | 1227.35 | 104.670 | 13.9923 | 1.78168 | 0.114634 | 0.0143402 |
| 7179.44 | 1227.35 | 104.670 | 13.9923 | 1.78168 | 0.114634 | 0.0143402 |
| 6670.79 | 1020.66 | 85.3333 | 10.6667 | 1.33333 | 0.085333 | 0.0106667 |
| 3482.72 | 893.007 | 60.9539 | 7.86972 | 0.99368 | 0.063786 | 0.0079767 |
| $\sim 10^{-12}$ | $\sim 10^{-13}$ | $\sim 10^{-13}$ | $\sim 10^{-14}$ | $\sim 10^{-15}$ | $\sim 10^{-17}$ | $\sim 10^{-18}$ |
| $\sim 10^{-12}$ | $\sim 10^{-13}$ | $\sim 10^{-13}$ | $\sim 10^{-14}$ | $\sim 10^{-16}$ | $\sim 10^{-17}$ | $\sim 10^{-18}$ |
| $\sim 10^{-12}$ | $\sim 10^{-13}$ | $\sim 10^{-13}$ | $\sim 10^{-14}$ | $\sim 10^{-17}$ | $\sim 10^{-18}$ | $\sim 10^{-18}$ |

As presented in Table 1, the three lowest eigenvalues are several orders of magnitude smaller than the remaining ones, which makes it possible to assume that they are of zero value. The eigenvectors associated with zero-value eigenvalues correspond to rigid body motions. The positive eigenvalues and corresponding eigenvectors are consistent with various states of plate deformation.

The above analysis shows that the considered finite element formulation complies with the ellipticity condition for a wide range of thicknesses.

### 3.2. Consistency condition

One of the forms of the consistency condition is the energy criterion. It is based on the following reasoning [1, 9]. The internal energy density $\tilde{E}_s$ can be represented in a differential form. In the FEM, this energy density can be written as a bilinear form $\tilde{E}_s^e$ with the use of finite element stiffness matrix and nodal displacements vector, divided by the element area. Each nodal displacement can be represented by its mean value and its derivatives in the form of a Taylor series. When the characteristic size of an element decreases to zero, only the first order (constant with respect to element dimensions) components remain. If they are the same as the corresponding components in $\widetilde{E}_s$, then we can say that the formulation is consistent. An analysis of the second and third order components provides information about the convergence of the formulation.

The density of the internal energy according to Hencky-Bollé plate theory is given by the following formula

$$\widetilde{E}_s = \frac{1}{2}\left[\begin{array}{l} D\left(\frac{\partial\phi_y}{\partial x}\right)^2 + D\left(\frac{\partial\phi_x}{\partial y}\right)^2 - 2D\nu\frac{\partial\phi_y}{\partial x}\frac{\partial\phi_x}{\partial y} + \frac{D(1-\nu)}{2}\left(\frac{\partial\phi_x}{\partial x} - \frac{\partial\phi_y}{\partial y}\right)^2 + \\ + H\left(\frac{\partial w}{\partial x} - \phi_y\right)^2 + H\left(\frac{\partial w}{\partial y} + \phi_x\right)^2 \end{array}\right] \tag{8}$$

The density of internal energy $\widetilde{E}_s^e$ accumulated in a finite element, can be written as a bilinear form

$$\widetilde{E}_s^e = \frac{1}{2}\frac{1}{4ab}\mathbf{q}^T\mathbf{K}^e\mathbf{q} \tag{9}$$

Let's express the nodal degrees of freedom with the use of Taylor series. The density of the finite element internal energy can then be written in the following way (without losing any details of the derivation we consider a rectangular element, with $a = b$)

$$\widetilde{E}_s^e = L_0(w,\phi_x,\phi_y;D,\nu) + aL_1(w,\phi_x,\phi_y;D,\nu) + a^2L_2(w,\phi_x,\phi_y;D,\nu) + \ldots, \tag{10}$$

with differential operators in the form

$$L_0 = \frac{1}{2}\left[\begin{array}{l} D\left(\frac{\Delta\phi_x}{\Delta x}\right)^2 + D\frac{1-\nu}{2}\left(\frac{\Delta\phi_x}{\Delta y}\right)^2 + D\left(\frac{\Delta\phi_y}{\Delta y}\right)^2 + D\frac{1-\nu}{2}\left(\frac{\Delta\phi_y}{\Delta x}\right)^2 + \\ + 2\nu D\frac{\Delta\phi_x}{\Delta x}\frac{\Delta\phi_y}{\Delta y} + (1-\nu)D\frac{\Delta\phi_y}{\Delta x}\frac{\Delta\phi_x}{\Delta y} + H\left[\left(\phi_x - \frac{\Delta w}{\Delta x}\right)^2 + \left(\phi_y - \frac{\Delta w}{\Delta y}\right)^2\right] \end{array}\right] \tag{11}$$

$$L_1 = 0$$

$$L_2 = \frac{1}{2}\left[\begin{array}{l} H\phi_x\left(\frac{\Delta^2\phi_x}{\Delta x^2}+\frac{\Delta^2\phi_x}{\Delta y^2}\right)+H\phi_x\left(\frac{\Delta^2\phi_y}{\Delta x^2}+\frac{\Delta^2\phi_y}{\Delta y^2}\right)+\frac{H}{3}\left(\frac{\Delta\phi_x}{\Delta x}\right)^2+\frac{H}{3}\left(\frac{\Delta\phi_x}{\Delta y}\right)^2+ \\ +\frac{H}{3}\left(\frac{\Delta\phi_y}{\Delta y}\right)^2+\frac{2}{3}\frac{\Delta^2\phi_x}{\Delta x^2}\left(\phi_y-\frac{\Delta w}{\Delta y}\right)+\frac{2}{3}\frac{\Delta^2\phi_y}{\Delta x^2}\left(\phi_x-\frac{\Delta w}{\Delta x}\right)+ \\ +\frac{H}{3}\left(\frac{\Delta\phi_y}{\Delta x}\right)^2+\frac{2H}{3}\left(\frac{\Delta\phi_x}{\Delta y}\right)\left(\frac{\Delta^2 w}{\Delta x\Delta y}\right)+\frac{2H}{3}\left(\frac{\Delta\phi_y}{\Delta x}\right)\left(\frac{\Delta^2 w}{\Delta x\Delta y}\right)+ \\ +\frac{2H}{3}\left(\frac{\Delta^2 w}{\Delta x\Delta y}\right)^2+\frac{D}{3}\left[\left(\frac{\Delta^2\phi_x}{\Delta x\Delta y}\right)+\left(\frac{\Delta^2\phi_y}{\Delta x\Delta y}\right)\right] \end{array}\right]$$

The analysis of the above expressions shows that the finite element formulation is consistent. When the element size $a \to 0$, only the first order entries remain and we get $\lim_{a\to 0}\tilde{E}_s^e = \tilde{E}_s$, as the differential operator $L_0$ represents the corresponding differential operator from the analytical plate model. The differential operator $L_1$ equals zero, which means that the order of convergence of the numerical model is quadratic. The presented differential operators don't depend on any small parameters, therefore no additional 'parasitic' energy can be generated when the ratio $h/a$ is small.

## 3.3. Inf-sup condition

### 3.3.1. The numerical procedure

The satisfaction of the inf-sup condition by a finite element formulation implies a monotonic and optimal convergence in bending-dominated problems. In formulations that conform to the criterion no parasitic states are observed even for very thin plates. As it is very difficult to verify this condition analytically, a numerical procedure was developed.

The algorithm of the numerical test is as follows. In each test case a sequence of several (usually up to four) finite element meshes with decreasing element size is chosen. For every $k$ ($k$=1,2,…,$n$) discretization in the sequence, an equation $\tilde{\mathbf{K}}_k\mathbf{q}_k = \lambda^k\mathbf{S}_k\mathbf{q}_k$ is solved, with specific stiffness $\tilde{\mathbf{K}}_k$ and norm $\mathbf{S}_k$ matrices, and the smallest eigenvalue $\lambda^k_{\min}$ is calculated. If $\lambda^k_{\min} = 0$ independently of the mesh density, the condition is not satisfied and therefore the discretization shows parasitic states. If, on the other hand, $\lambda^k_{\min} > 0$ for the coarsest mesh, it should be verified if there is any dependence of the lowest non-zero eigenvalue on the characteristic mesh size. Usually it is done by creating and examining a graph of $\log\left(\lambda_{\min}^{k}\right)$ in function of $\log\left(1/N^{k}\right)$. If the curve quickly flattens and $\lambda_{\min}^{k}$ converges to a positive value, it is said that the condition is satisfied.

The selection of the stiffness matrix $\widetilde{\mathbf{K}}_{k}$ depends on the type of the analyzed finite element formulation. In a standard displacement formulation, it is the full, unchanged stiffness matrix of a finite element. The norm matrix **S** depends on the problem in question. The solution of the problem described in this paper belongs to the Sobolev space. In the internal energy expression there are components of displacements and their first derivatives, therefore the $H^1$ norm should be used. In the paper [19] the authors proposed a simplification, which assumed that $L^2$ norm can be used instead, as the solutions in both cases don't exhibit any qualitative differences. Due to the fact that the norm matrix corresponding to $L^2$ norm conforms to the mass matrix of an element with unit mass density, the eigenproblem considered is transformed into a simple frequency analysis.

The satisfaction of the inf-sup condition by the finite element formulation is analyzed with consideration of various cases. We study the influence of different boundary conditions, and two types of norm matrices $\mathbf{S}_{k}$ (corresponding to $H^1$ and $L^2$ norms accordingly) on the inf-sup test results.

The computations are performed in ABAQUS/Standard software with the use of the user element subroutine, which makes it possible to include own finite element formulations. The finite element stiffness matrix and the norm matrices are coded in FORTRAN programming language in a separate file with a structure required by the software. The subroutine is called by an input file, in which the problem geometry, boundary conditions and other simulation parameters are defined.

### 3.3.2. THE NORM MATRICES

The $L^2$ norm for the plate finite element is expressed as following

$$\left\|\overline{\mathbf{u}}\right\|_0^2 = \int_V \left(\overline{u}^{\,2} + \overline{v}^{\,2} + \overline{w}^{\,2}\right) \mathrm{d}V = \int_\Omega \left(hw^2 + \frac{h^3}{12}\phi_x^2 + \frac{h^3}{12}\phi_y^2\right) \mathrm{d}\Omega = \int_\Omega \mathbf{u}^T \mathbf{n}_0 \mathbf{u} \,\mathrm{d}\Omega \tag{12}$$

where

$$\mathbf{u}(x,y) = [w \ \phi_x \ \phi_y]^{\mathrm{T}}, \ \mathbf{n}_0 = diag\left[h, \frac{h^3}{12}, \frac{h^3}{12}\right]. \tag{13}$$

As it was mentioned before, the norm matrix obtained from the above equation is identical to a mass matrix of an element with unit material density

$$\mathbf{S}_0 = \int_\Omega \mathbf{N}^T \mathbf{n}_0 \mathbf{N} \mathrm{d}\Omega, \tag{14}$$

where **N** are displacement shape functions.

It was shown in [24, 25] that matrix $\mathbf{S}_0$ is positive definite, which allows us to use standard FEM procedures to solve the eigenproblem. If we take $\mu_0 = h,\ \mu_2 = h^3/12$, then the entries of the matrix

$$\mathbf{S}_0 = \left[\mathbf{S}_{ij}\right],\ \mathbf{S}_{ij} = \left[s_{oij}^{kl}\right]\ (i,j = 1,2,3,4,\ k,l = 1,2,3) \tag{15}$$

are as follows

$$\begin{aligned} s_{0ij}^{11} &= \mu_0 ab\left[\frac{1}{2} + \frac{\xi_i\xi_j}{210}\left(51 - 18\mu_x + 2\mu_x^2\right)\right]\left[\frac{1}{2} + \frac{\eta_i\eta_j}{210}\left(51 - 18\mu_y + 2\mu_y^2\right)\right] + \\ &+ \mu_2 \frac{3b}{5a}\xi_i\xi_j\left(1-\mu_x\right)^2\left[\frac{1}{2} + \frac{\eta_i\eta_j}{210}\left(51 - 18\mu_y + 2\mu_y^2\right)\right] + \\ &+ \mu_2 \frac{3a}{5b}\eta_i\eta_j\left(1-\mu_y\right)^2\left[\frac{1}{2} + \frac{\xi_i\xi_j}{210}\left(51 - 18\mu_x + 2\mu_x^2\right)\right], \end{aligned} \tag{16}$$

$$\begin{aligned} s_{0ij}^{12} &= \mu_0 a^2 b\left[\frac{1}{6}\xi_j + \frac{\xi_i}{210}\left(9 - 11\mu_x + 2\mu_x^2\right)\right]\left[\frac{1}{2} + \frac{\eta_i\eta_j}{210}\left(51 - 18\mu_y + 2\mu_y^2\right)\right] + \\ &+ \mu_2 \frac{b\xi_i}{10}\left(1 - 7\mu_x + 6\mu_x^2\right)\left[\frac{1}{2} + \frac{\eta_i\eta_j}{210}\left(51 - 18\mu_y + 2\mu_y^2\right)\right] + \\ &+ \mu_2 \frac{3a^2}{5b}\eta_i\eta_j\left(1-\mu_y\right)^2\left[\frac{1}{6}\xi_j + \frac{\xi_i}{210}\left(9 - 11\mu_x + 2\mu_x^2\right)\right], \end{aligned}$$

$$\begin{aligned} s_{0ij}^{13} &= \mu_0 b^2 a\left[\frac{1}{6}\eta_j + \frac{\eta_i}{210}\left(9 - 11\mu_y + 2\mu_y^2\right)\right]\left[\frac{1}{2} + \frac{\xi_i\xi_j}{210}\left(51 - 18\mu_x + 2\mu_x^2\right)\right] + \\ &+ \mu_2 \frac{a\eta_i}{10}\left(1 - 7\mu_y + 6\mu_y^2\right)\left[\frac{1}{2} + \frac{\xi_i\xi_j}{210}\left(51 - 18\mu_x + 2\mu_x^2\right)\right] + \\ &+ \mu_2 \frac{3b^2}{5a}\xi_i\xi_j\left(1-\mu_x\right)^2\left[\frac{1}{6}\eta_j + \frac{\eta_i}{210}\left(9 - 11\mu_y + 2\mu_y^2\right)\right], \end{aligned}$$

$$s_{0ij}^{22} = \mu_0 a^3 b\left[\frac{1}{15}\xi_i\xi_j + \frac{1}{105}(1-\mu_x)^2\right]\left[\frac{1}{2} + \frac{\eta_i\eta_j}{210}\left(51-18\mu_y+2\mu_y^2\right)\right] +$$
$$+\mu_2 ab\left[\frac{1}{6}\xi_i\xi_j + \frac{1}{10}\left(1-2\mu_x+6\mu_x^2\right)\right]\left[\frac{1}{2} + \frac{\eta_i\eta_j}{210}\left(51-18\mu_y+2\mu_y^2\right)\right] +$$
$$+\mu_2\frac{3a^3}{5b}\eta_i\eta_j(1-\mu_y)^2\left[\frac{1}{15}\xi_i\xi_j + \frac{1}{105}(1-\mu_x)^2\right],$$

$$s_{0ij}^{23} = \mu_0 a^2 b^2\left[\frac{1}{6}\xi_i + \frac{\xi_j}{210}\left(9-11\mu_x+2\mu_x^2\right)\right]\left[\frac{1}{6}\eta_i + \frac{\eta_j}{210}\left(9-11\mu_y+2\mu_y^2\right)\right] +$$
$$+\mu_2\frac{b^2\xi_i}{10}\left(1-7\mu_x+6\mu_x^2\right)\left[\frac{1}{6}\eta_j + \frac{\eta_i}{210}\left(9-11\mu_y+2\mu_y^2\right)\right] +$$
$$+\mu_2\frac{a^2\eta_i}{10}\left(1-7\mu_y+6\mu_y^2\right)\left[\frac{1}{6}\xi_j + \frac{\xi_i}{210}\left(9-11\mu_x+2\mu_x^2\right)\right],$$

$$s_{0ij}^{33} = \mu_0 a b^3\left[\frac{1}{15}\eta_i\eta_j + \frac{1}{105}(1-\mu_y)^2\right]\left[\frac{1}{2} + \frac{\xi_i\xi_j}{210}\left(51-18\mu_x+2\mu_x^2\right)\right] +$$
$$+\mu_2 ab\left[\frac{1}{6}\eta_i\eta_j + \frac{1}{10}\left(1-2\mu_y+6\mu_y^2\right)\right]\left[\frac{1}{2} + \frac{\xi_i\xi_j}{210}\left(51-18\mu_x+2\mu_x^2\right)\right] +$$
$$+\mu_2\frac{3b^3}{5a}\xi_i\xi_j(1-\mu_x)^2\left[\frac{1}{15}\eta_i\eta_j + \frac{1}{105}(1-\mu_y)^2\right],$$

$$s_{0ij}^{21} = \xi_i\xi_i s_{0ij}^{12}, \quad s_{0ij}^{31} = \eta_i\eta_j s_{0ij}^{13}, \quad s_{0ij}^{32} = \xi_i\xi_i\eta_i\eta_j s_{0ij}^{23}.$$

The first order norm is defined as

$$\|\bar{\mathbf{u}}\|_1^2 = \int_V \left(\Delta\bar{u}^2 + \Delta\bar{v}^2 + \Delta\bar{w}^2\right)\mathrm{d}V =$$
$$= \int_\Omega \left[\frac{h^3}{12}\left(\frac{d\phi_x}{dx}\right)^2 + \frac{h^3}{12}\left(\frac{d\phi_x}{dy}\right)^2 + h\phi_x^2 + \frac{h^3}{12}\left(\frac{d\phi_y}{dx}\right)^2 + \frac{h^3}{12}\left(\frac{d\phi_y}{dy}\right)^2 + h\phi_y^2 + h\left(\frac{dw}{dx}\right)^2 + h\left(\frac{dw}{dy}\right)^2\right]d\Omega \quad (17)$$
$$= \int_\Omega \tilde{\mathbf{u}}^T \mathbf{n}_1 \tilde{\mathbf{u}}\; d\Omega$$

where

$$\tilde{\mathbf{u}}(x,y)=\left[\frac{dw}{dx}\ \ \frac{dw}{dy}\ \ \frac{d\phi_x}{dx}\ \ \frac{d\phi_x}{dy}\ \ \frac{d\phi_y}{dx}\ \ \frac{d\phi_y}{dy}\ \ \phi_x\ \phi_y\right]^T,\ \mathbf{n}_1=diag\left[h,h,\frac{h^3}{12},\frac{h^3}{12},\frac{h^3}{12},\frac{h^3}{12},h,h\right] \tag{18}$$

Norm matrix $\mathbf{S}_{01}$ representing this norm is calculated from

$$\mathbf{S}_{01}=\int_{\Omega}\mathbf{N}_1^T\mathbf{n}_1\mathbf{N}_1 d\Omega+\mathbf{S}_0 \tag{19}$$

The norm matrix $\mathbf{S}_{01}$ based on displacements and their derivatives is also positive definite. The elements of the matrix are of substantial size, therefore they are not presented in the paper.

#### 3.3.3. The test cases

The benchmark cases chosen to test the considered finite element are square plates with the following boundary conditions: (a) clamped on one edge, (b) clamped on all edges and (c) simply supported on all edges. In the paper [18] the author analyzed these cases in order to establish the percentage of bending part in total energy. The study showed that in the cantilever and simply supported plate cases the bending energy prevails for the entire considered range, $h/2a \in (0, 0.5]$. For the clamped plate case the bending part is higher than 50% up to $h/2a$=0.31.

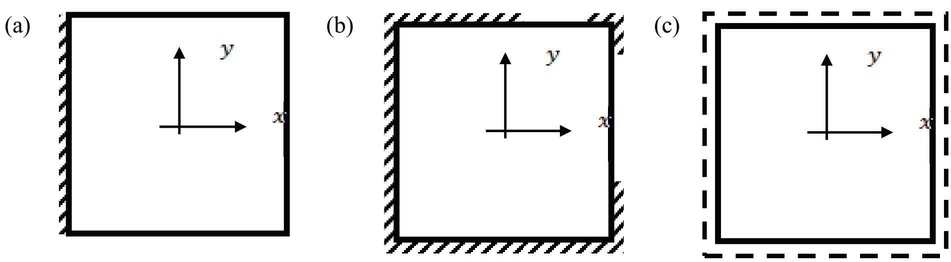


Fig. 2. The benchmark cases, a) clamped plate, b) cantilever plate, c) simply supported plate

The inf-sup condition graphs for ratio $h/2a$ = 1/5, 1/20, and 1/100, are presented in Fig. 3, Fig. 4 and Fig. 5 accordingly. The discretizations used are: 2 by 2, 4 by 4, 8 by 8, and 16 by 16 finite elements. An eigenvalue problem was solved for each mesh and the lowest eigenvalue was monitored. The figures show a comparison of convergence curves for $\lambda_{min}$ in the logarithmic scale, $\log(\lambda_{min})$ vs. $\log(1/N)$, obtained with the use of stiffness matrix $\mathbf{K}$ and norm matrices $\mathbf{S}_0$ and $\mathbf{S}_{01}$.

(a)

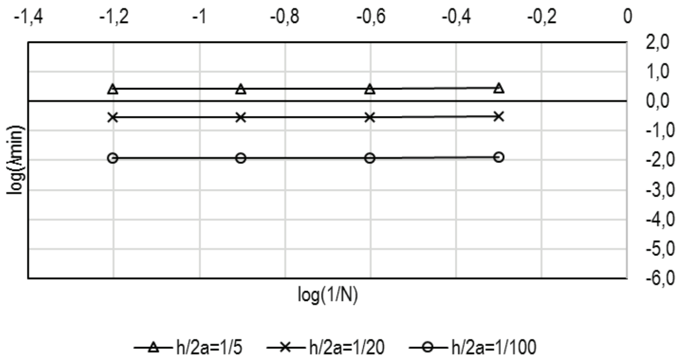


(b)

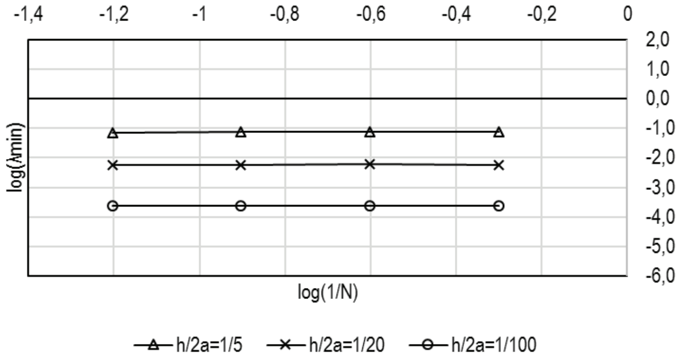


Fig. 3. The inf-sup condition graphs for the clamped plate, with the use of (a) S0, and (b) S01 norm matrices

(a)

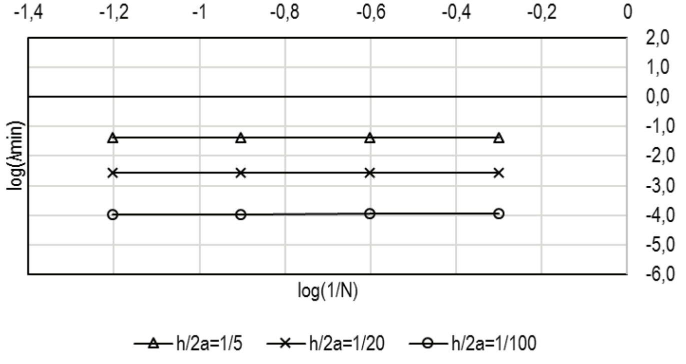

(b)

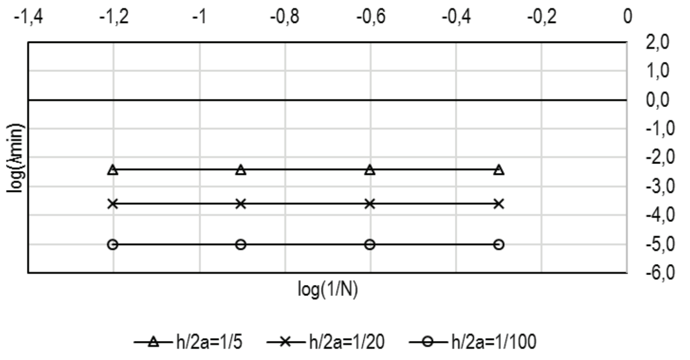


Fig. 4. The inf -sup condition graphs for the cantilever plate, with the use of (a) S0, and (b) S01 norm matrices

(a)

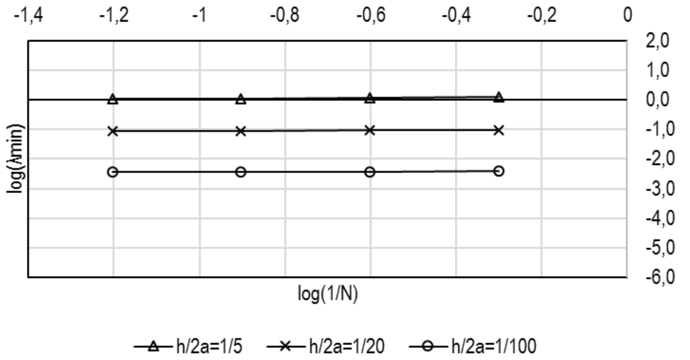


(b)

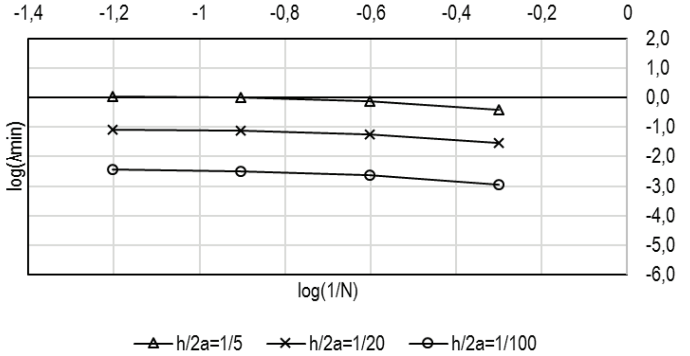


Fig. 5. The inf -sup condition graphs for the simply supported plate, with the use of (a) S0, and (b) S01 norm matrices

The plate finite element satisfies the inf-sup condition in every test case when the full stiffness matrix is used, along with both norm matrices $\mathbf{S}_0$ and $\mathbf{S}_{01}$. The plots are almost flat in the considered range of the $h/2a$ aspect ratio, which shows that the solution is stable and independent from the mesh density.

## 4. CONCLUDING REMARKS

The plate finite element with physical shape functions satisfies: ellipticity, consistency and inf-sup conditions, which means that its formulation is correct. Fulfillment of the ellipticity condition guarantees existence and uniqueness of FEM solution. When consistency and inf-sup conditions are met, it implies that the convergence of the finite element solution to the exact one is monotonic. The finite element considered in this paper is free from locking, and no additional zero-energy states are present when element thickness tends to zero.

To conclude, the finite element is theoretically correct. Numerical results presented in [6] are then confirmed by the theoretical analysis.

## REFERENCES

1. Gilewski W., *On the criteria for evaluation of finite elements – from Timoshenko beam to Hencky-Bolle plate*. (in Polish) Warsaw University of Technology Publishing House (OWPW): Warsaw, 2005.
2. Gilewski W., Radwańska M., A survey of finite element models for the analysis of moderately thick shells. *Finite Element Analysis and Design* 1991; **9**:1-21.
3. Radwańska M., An overview of selected plate and shell finite element models with graphic presentation of geometric equation. *Comp. Ass. Mech. Eng. Sc*. 2007; **14**:431-456.
4. Witkowski W., 4-node combined shell element with semi-EAS-ANS strain interpolations in 6-parameter shell theories with drilling degrees of freedom. *Comp. Mech*. 2009; **43**(2):307-319.
5. Kączkowski Z., *Plates-static calculations.* (in Polish) Arkady: Warsaw, 1980.
6. Gilewski W., Gomuliński A., Physical shape functions in finite element analysis of moderately thick plates. *Int. Journ. Num. Meth. Engrg*. 1991; **32**:1115-1136.
7. Bathe K.J., Dvorkin E., A formulation of general shell elements – The use of mixed interpolation of tensorial components. *Int. J. Num. Meth. Eng.* 1986; **22**:697-722.
8. Bathe K.J., The inf-sup condition and its evaluation for mixed finite element methods. *Comp. Struct.* 2001; **79**:243-252.
9. Gilewski W., A simple method for the analysis of correctness of FEM formulations. *Computational Mechanics. Theory and Applications*, 1995; **1**:678-683.
10. Brezzi F., On existence, uniqueness and approximation of saddle-point problems arising from Lagrangian multipliers. *RAIRO, Anal. Numer*. 1974; **8**:129-151.
11. Babuska I., The finite element method with Lagrange multipliers. *Num. Math.* 1977; **20**: 322-333.
12. Chapelle D., Bathe K.J., The inf-sup test. *Computers and Structures*. 1993; **47**:537-545.
13. Bathe K.J., *Finite element procedures*. Prentice Hall: Engelwood Cliffs, NJ, 1996.
14. Bathe K.J., Iosilevich A., Chapelle D., An evaluation of the MITC shell elements. *Comp. Struct.* 2000; **75**: 1-30.
15. Berkovic M., Mijuca D., Grozdanovic I., Some continuous stress mixed formulations and inf-sup test. *Comp. Ass. Mech. Eng. Sci*. 2001; **8**:141-153.

16. Kirmse A., Bending-dominated deformations of thin spherical shells: Analysis and finite-element approximation. *SIAM J. Numer. Anal*. 1993; **30**:1015-1040.
17. Pitkaranta J., Sanchez-Palencia E., On the asymptotic behavior of sensitive shells with small thickness. *C. R. Acad. Sci. Paris* 1997; **325**:127-134.
18. Chapelle D., Bathe K.J., Fundamental considerations for the finite element analysis of shell structures. *Comp. Struct.* 1998; **66**:19-36.
19. Gilewski W., Sitek M., The inf-sup condition tests for shell/plate finite elements, *Archives of Civil Engrg*. 2011; **57**(4):425-447.
20. Iosilevich A., Bathe K.J., Brezzi F., On evaluating the inf-sup condition for plate bending elements. *Int. Journ. Num. Meth. Engrg*. 1997; **40**:3639-3663.
21. Hencky H., Uber die berűcksichtigung der schubverzerrung in ebenen platen. *Ingenieur-Archiv*. 1947; **16**(1):72-76.
22. Bollé L., Contribution un problème linéaire de flexion d'un plaque elastique. *Bulletin Techniqué de la Suisse Romande* 1947; **73**(21-22):281-285&293-298.
23. Reissner E., Reflections on the theory of elastic plates. *Applied Mechanics Review* 1985; **38**(11):1453-1464.
24. Gilewski W., Sitek M., Evaluation of shell finite elements: ellipticity, consistency and inf-sup condition. Some practical examples. CMM-2007, Łódź-Spała 2007.
25. Sitek M., *Correctness assessment of beam, plate and shell finite elements*, PhD Thesis (in Polish) Warsaw University of Technology Publishing House (OWPW): Warsaw, 2010.

*Received 24.06.2017*

*Revised 30.08.2017*

## LIST OF FIGURES AND TABLES

# PŁYTOWY ELEMENT SKOŃCZONY O FIZYCZNYCH FUNKCJACH KSZTAŁTU: POPRAWNOŚĆ SFORMUŁOWANIA

*Słowa kluczowe: płytowy element skończony, fizyczne funkcje kształtu, eliptyczność, zgodność, warunek inf-sup.*

**STRESZCZENIE:**

Przedmiotem pracy jest weryfikacja poprawności sformułowania prostokątnego płytowego element skończonego o tzw. fizycznych funkcjach kształtu. Sformułowanie fizycznych funkcji kształtu bazuje na teorii płyt o średniej grubości Hencky-Bollé'a. Funkcje te w zagadnieniu dwuwymiarowym otrzymywane są jako superpozycja rozwiązań otrzymanych dla dwóch krzyżujących się pasm płytowych i bazują na rozwiązaniach odpowiednich równań różniczkowych zwyczajnych. Fizyczne funkcje kształtu są czułe na zmiany parametrów fizycznych i geometrycznych elementu skończonego. Płytowy element skończony znany jest od dawna, lecz jego dobre własności zbieżności dla różnych parametrów geometrycznych wykazane były jedynie na przykładach testowych. Sformułowanie to jest niestandardowe w zakresie metody elementów skończonych i nie można zastosować klasycznych technik oceny poprawności formułowania i zbieżności rozwiązań MES. W pracy wykazano poprawność rozważanego elementu skończonego na podstawie kryteriów eliptyczności i zgodności, oraz warunku inf-sup, które zaproponowano w latach 90-tych XX wieku dla sformułowań mieszanych MES. Spełnienie tych kryteriów zapewnia istnienie jednoznacznego rozwiązania, stabilność rozwiązania i optymalną zbieżność do rozwiązania dokładnego.

Sprawdzenie kryterium eliptyczności polega na analizie wartości i wektorów własnych macierzy sztywności pojedynczego elementu skończonego. Macierz sztywności elementu prostokątny o fizycznych funkcjach kształtu ma dla dowolnych parametrów geometrycznych trzy zerowe wartości własne, którym odpowiadają ruchy sztywne elementu. Pozostałe dziewięć wartości własnych jest dodatnich i odpowiadają im wektory własne, które generują odkształcenia elementu. Element spełnia tym samym warunek istnienia i jednoznaczności rozwiązania zadania MES.

Sprawdzenie warunku zgodności bazuje na kryterium energetycznym, w myśl którego porównuje się gęstość energii odkształcenia w sformułowaniu rozważanej teorii płyt oraz odpowiedniego sformułowania MES. Postać gęstości energii odkształcenia w ujęciu MES pozwala zdefiniować człony związane z tzw. stanami pasożytniczymi energii, które mogą zależeć od parametrów geometrycznych lub fizycznych płyty i występują w wielu elementach skończonych. W płytach o średniej grubości najczęściej występuje stan pasożytniczy związany z poprzecznym ścinaniem, który zaburza wyniki obliczeń przy obliczeniach dźwigarów cienkich. W analizowanym elemencie skończonym postać wyrażenia na energię potencjalną jest poprawna i nie zawiera żadnych członów pasożytniczych. Oznacza to, że rozwiązanie zadania MES jest stabilne zarówno dla płyt o średniej grubości jak i cienkich.

Analityczne sprawdzenie warunku inf-sup jest bardzo złożone i rzadko stosowane w literaturze. W latach 90-tych XX wieku zaproponowano numeryczny sposób weryfikacji tego warunku i tak właśnie analizowano rozważany element skończony. Warunek inf-sup, w odróżnieniu od poprzednich dwóch warunków, należy badać w specjalnie wybranych zadaniach dla układów wielu elementów skończonych. Weryfikacja numeryczna polega na badaniu zbieżności najmniejszej wartości własnej uogólnionego zagadnienia własnego w którym występuje macierz sztywności układu elementów i specjalnie dobrana macierz normowa. W pracy przedstawiono analityczną postać wzorów na macierze normowe. Zbieżność rozwiązania badano dla trzech typowych warunków podparcia płyty, uzyskując znakomitą zbieżność rozwiązania inf-sup, która gwarantuje optymalną zbieżność rozwiązań zadań MES.

Płytowy element skończony o fizycznych funkcjach kształtu bez zastrzeżeń spełnia wszystkie wymagane kryteria, co stanowi teoretyczne potwierdzenie jego przydatności do analizy płyt o średniej grubości i cienkich.